values are changed by neutral substituents on the 1,2,3-triazole ring but are not affected by charged carboxyl groups. This point is illustrated if one compares the pK values of 4,5-dibromo-1,2,3-triazole and the carboxyl-substituted triazoles with the pK value of triazole (Table III). The carboxyl anions on the 4,5-dicarboxylic acid have no effect on the pK for the ionization of the N–H proton. In contrast, the pK for 4,5-dibromo-1,2,3-triazole is lowered considerably by the bromine substituents in the ring. These facts can be explained by noting that the entropy change for the ionization from the N–H group in the dicarboxylic acid derivative is about three times as great as the entropy change for ionization from 1,2,3-triazole because the proton ionizes in the field of three charges. This fortuitously offsets the decrease in the enthalpy change and the free energy is not affected. In the case of the dibromo derivative, the entropy change is the same as that for triazole and, hence, the decrease in the enthalpy change decreases the free energy change.

Further studies are now being conducted in this laboratory to attempt to determine the mechanism of the very large substituent affect on ΔH° for proton ionization from the 1,2,3-triazole ring.

Acknowledgments. The authors wish to thank Drs. Reed M. Izatt and J. J. Christensen, Brigham Young University, for the use of their equipment for part of this study and for many helpful discussions.

A Study of the Kinetics of the Oxidation of Arsenic(III) by Electrogenerated Iodine in Alkaline Media

D. C. Johnson and Stanley Bruckenstein[1]

Contribution from the Department of Chemistry, University of Minnesota, Minneapolis, Minnesota 55455. *Received May 20, 1968*

Abstract: The oxidation of As(III) by electrogenerated I_3^- was studied in aqueous media for $8.17 \leq pH \leq 9.17$ using the rotating ring-disk electrode. On the basis of chemical kinetic evidence reported in the literature, it is shown that the mechanism commonly given to account for the observed rate law at low pH is not correct for pH >7. The rate of oxidation of all forms of As(III) is given by $-d[As(III)]/dt = k[I_3^-][H_2AsO_3^-] + k'[I_2][H_2AsO_3^-]$ where $k = (5.65 \pm 0.05) \times 10^6$ l. mol^{-1} sec^{-1} and $k' = (1.75 \pm 0.15) \times 10^8$ l. mol^{-1} sec^{-1}.

The purpose of this research was to investigate the kinetics of the reaction between iodine and As(III) in aqueous solutions of pH >7. Roebuck[2,3] reported the forward rate law for the reaction

$$H_2O + H_3AsO_3 + I_3^- \underset{}{\overset{k_f}{\rightleftharpoons}} H_3AsO_4 + 3I^- + 2H^+ \quad (1)$$

in acidic media to be

$$\frac{-d[As(III)]}{dt} = \frac{k_f[As(III)][I_3^-]}{[I^-]^2[H^+]} = k_{obsd}[As(III)][I_3^-] \quad (2)$$

where $k_f = 1.57 \times 10^{-5}$ mol^2 l.$^{-2}$ sec^{-1}.[4]

The mechanism suggested by Liebhafsky[5] to account for the observed rate law at low pH is

$$I_3^- + H_2O \rightleftharpoons HIO + H^+ + 2I^- \quad (3)$$

$$HIO + H_3AsO_3 \overset{k_f}{\rightleftharpoons} H_3AsO_4 + H^+ + I^-$$

On the basis of this mechanism[6] and other data,[7,8] it has been suggested that the kinetic behavior of halogens in aqueous media can usually be explained by a mechanism involving the hypohalous acid or anion.

Eigen and Kustin[9] determined the forward rate constant for disproportionation of I_2 using temperature-jump methods. They report $k_f = 3$ sec^{-1} for the reaction

$$I_2 + H_2O \underset{k_b}{\overset{k_f}{\rightleftharpoons}} HIO + H^+ + I^-$$

Combining this result with the dissociation constant for I_3^-, 1.4×10^{-3}, and neglecting k_b, permits one to calculate the maximum rate of production of HIO according to eq 4. However, it is well known that the

$$\frac{d[HIO]}{dt} = \frac{4.2 \times 10^{-3}[I_3^-]}{[I^-]} \quad (4)$$

I_3^-–As(III) reaction is extremely rapid in alkaline media, in conflict with the result predicted by eq 4 for the usual values of the ratio $[I_3^-]/[I^-]$. Thus, the oxidation of As(III) by I_3^- in alkaline media must occur by some mechanism other than that proposed by Liebhafsky for acid media.

A steady-state electrochemical technique, using the rotating ring-disk electrode (rrde), was selected to study this reaction. The rrde has been applied to the study of second-order homogeneous reactions where the reaction is diffusion[10–12] or kinetically[13] controlled.

(1) Author to whom inquiries should be addressed at the Department of Chemistry, State University of New York at Buffalo, Buffalo, N. Y. 14214.
(2) J. R. Roebuck, *J. Phys. Chem.*, **6**, 365 (1902).
(3) J. R. Roebuck, *ibid.*, **9**, 727 (1905).
(4) H. A. Liebhafsky, *J. Am. Chem. Soc.*, **61**, 3513 (1939).
(5) H. A. Liebhafsky, *J. Phys. Chem.*, **35**, 1648 (1931).
(6) W. M. Latimer, "The Oxidation States of the Elements and Their Potentials in Aqueous Solutions," Prentice-Hall, Inc., Englewood Cliffs, N. J., 1952, p 115.
(7) W. C. Bray, *Z. Phys. Chem.*, **54**, 463 (1906).
(8) B. Makower and H. A. Liebhafsky, *Trans. Faraday Soc.*, **29**, 597 (1933).
(9) M. Eigen and K. Kustin, *J. Am. Chem. Soc.*, **84**, 1355 (1962).
(10) S. Bruckenstein and D. C. Johnson, *Anal. Chem.*, **36**, 2186 (1964).

The principle upon which this technique is based depends on the electrochemical generation of an oxidant (I_3^-) from excess of some species present in the supporting electrolyte (I^-) at the disk electrode and the subsequent reaction of this oxidant with the reductant (As(III)) in the convective diffusion layer between the disk and ring electrodes. The rate of production of oxidant is controlled by the current through the disk electrode and any unreacted oxidant is detected amperometrically at the ring electrode. The rate constant for the reaction of the oxidant and reductant can be calculated from the imposed disk electrode current, I_d, and the detected ring electrode current, I_r.[13]

At a particular disk current, in excess of the diffusion controlled flux of As(III) to the disk electrode, there exist three zones. As one moves outward in a radial direction from the axis of rotation for the rrde, one encounters a zone containing I_3^-, As(V), and virtually no As(III); a reaction zone with comparable amounts of these species; and finally a zone in which there is only As(III). The reaction front is defined as that surface in the reaction zone where [As(III)] = $[I_3^-]$.

At a value of disk current such that the radial coordinate of the reaction front at the electrode surface, R_J, is equal to the inner radius of the ring, R_2, a ring current, I_r ($R_J = R_2$), will be observed which is inversely proportional to the pseudo-second-order rate constant, k_{obsd} (eq 2), of the homogeneous reaction.[13] This current is

$$I_r(R_J = R_2) = BnF\pi R_2^2 D\omega^{3/2}\nu^{-1/2}k_{obsd}^{-1} \qquad (5)$$

where ω is the angular velocity of electrode rotation, ν is the kinematic viscosity of the solution, D is the diffusion coefficient of the reaction species, the product, nF, has its usual electrochemical significance, and B is a numerical constant. B was previously calculated[13] to be 590 (I_r measured in μA). Albery has recently given a more general derivation for the kinetic ring current, $I_r(R_J = R_2)$.[14] The new solution has the same form as eq 5 with B equal to 210. The latter value was used for all calculations reported in this paper.

Experimental Section

Instrumentation. The rrde used in this research was constructed of platinum and Teflon by Pine Instruments of Grove City, Pa. according to a procedure described elsewhere.[15,16] Following each experiment (~0.5 hr) the electrode surface was polished lightly using 0.05-μ alumina on Buehler microcloth. For this electrode R_1 = 0.3820 cm, R_2 = 0.3980 cm, R_3 = 0.4220 cm, α = 0.131, $\beta^{2/3}$ = 0.361, and N = 0.183.

The instrumentation originally described for diffusion layer titrations[11] was altered because no satisfactory method existed for direct measurement of the imposed disk current. The revised schematic is shown in Figure 1. The circuit for current control in the disk electrode is comprised of control amplifier A-1 and voltage follower F-1. If resistors R_1 and R_2 are equal, the control amplifier

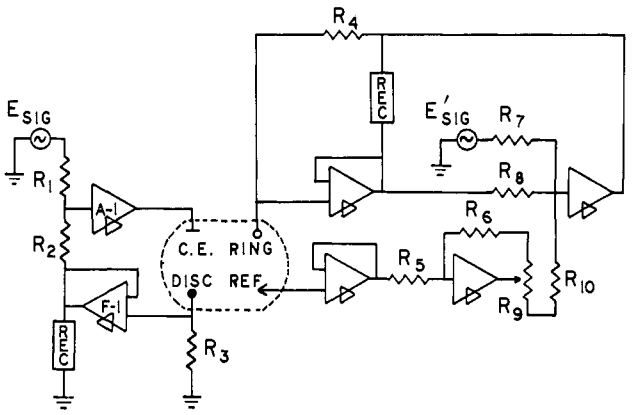

Figure 1. Schematic diagram of instrument: C.E. = platinum counter electrode isolated from bulk solution by fritted glass; R_1, R_2, R_5, R_6, R_7, R_8, R_{10} = resistors, 100 K, 1%; R_3 = current-measuring resistor for disk electrode, 1 K to 1 Megohm, 1%; R_4 = current-measuring resistor for ring electrode, 10–20 K, 1%; R_9 = potentiometer, 30 turn, 5 K.

functions to maintain the relationship $E_{sig} = -I_dR_3$. E_{sig} was provided by a conventional ramp signal generator.

The remaining circuitry in Figure 1 provides potential control for the ring electrode. The operation of this circuitry has been described elsewhere.[17]

Titration curves were recorded using a Houston Omnigraphic HR-97 X-Y recorder.

All experiments were performed in a water-jacketed cell at a temperature of 25.0 ± 0.2°. Solutions were bubbled using Linde L 3 nitrogen which had been presaturated with H_2O. During titrations, a nitrogen atmosphere was maintained over the solution. The counter electrode was a platinum electrode placed in a fritted glass compartment containing 5.0 M $NaClO_4$. The reference potential was supplied by a sce in electrical contact with the solution through a Luggin capillary containing saturated $NaNO_3$ solution. The tip of the Luggin capillary was placed less than 3 mm from the surface of the ring electrode to compensate for the majority of cell resistance. The potential of the ring electrode was maintained at +0.1 V *vs.* sce.

Chemicals. Standard solutions of As(III) (0.5000 M) were prepared by dissolving Mallinckrodt Primary Standard As_2O_3 in approximately 1 M NaOH solution. This solution was kept in a tightly capped volumetric flask and, over the time period encompassed by our experiments, the change in As(III) concentration was negligible.

The buffer used for pH control was the H_3BO_3–$H_2BO_3^-$ system. The appropriate amount of a 0.500 M stock solution of Mallinckrodt H_3BO_3 was added to the supporting electrolyte solution and a standard solution of Mallinckrodt Analytical Reagent NaOH added to adjust pH. Unless stated otherwise, $[H_3BO_3] + [H_2BO_3^-]$ = 0.050 M.

The ionic strength of the solutions was maintained at 0.50 M by addition of 5.00 M $NaClO_4$ solution. The stock $NaClO_4$ was prepared by neutralizing Mallinckrodt Analytical Reagent NaOH with Mallinckrodt Analytical Reagent $HClO_4$ to pH 7.

The pH of the titration solutions was measured using a Beckman Model H pH meter calibrated with Mallinckrodt pH 7.00 and 10.00 Buffar solutions.

All other chemicals used were Baker Analyzed Reagent grade.

Interpretation of $I_r - I_d$ Curves. The effect of kinetics upon the curvature of an experimental plot of I_r *vs.* I_d is minimal for low values of rotation speed.[13] For I_d such that $R_J > R_3$, the titration curve is described by eq 6.[12]

$$I_r = -NI_d - M\beta^{2/3} \qquad (6)$$

$$M = 620nF\pi R_1^2 D^{2/3}\omega^{1/2}\nu^{-1/6}C^b \qquad (7)$$

where C^b is the bulk concentration of As(III) in moles liter^{-1}. The intersection of the extrapolated linear portion of the titration curve with the residual ring current (I_r = 0) yields the disk current,

(11) W. J. Albery, S. Bruckenstein, and D. C. Johnson, *Trans. Faraday Soc.*, **62**, 1938 (1966).
(12) D. C. Johnson, Ph.D. Thesis, University of Minnesota, Minneapolis, Minn., 1967.
(13) W. J. Albery and S. Bruckenstein, *Trans. Faraday Soc.*, **62**, 2584 (1966).
(14) W. J. Albery, private communication.
(15) W. J. Albery and S. Bruckenstein, *Trans. Faraday Soc.*, **62**, 1920 (1966).
(16) D. C. Johnson, D. T. Napp, and S. Bruckenstein, *Anal. Chem.*, **40**, 482 (1968).
(17) D. T. Napp, D. C. Johnson, and S. Bruckenstein, *ibid.*, **39**, 481 (1967).

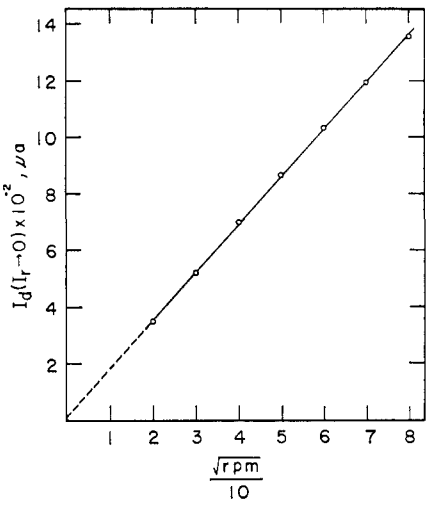

Figure 2. $I_d(I_r \to 0)$ *vs.* $\sqrt{\text{rpm}}$: [As(III)] = 5.00×10^{-4} *M*, [NaI] = 0.060 *M*, μ = 0.50 *M*, pH 8.67.

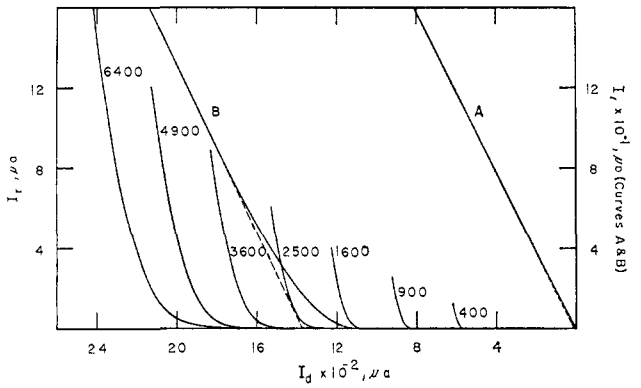

Figure 3. I_r–I_d curves: curve A, [As(III)] = 0 *M*, 1600 rpm, right I_r axis; curve B, [As(III)] = 1.00×10^{-3} *M*, 1600 rpm, right I_r axis; remaining curves, [As(III)] = 1.00×10^{-3} *M*, rpm values given on curve, left current axis; $a_{H^+} = 6.61 \times 10^{-9}$ *M*, [NaI] = 0.070 *M*.

$I_d(I_r \to 0)$. From eq 6

$$I_d(I_r \to 0) = -M\beta^{2/3}/N \tag{8}$$

The disk current when $R_J = R_2$, $I_d(R_J = R_2)$, is related to *M* by[11]

$$I_d(R_J = R_2) = -M/[1 - F(\alpha)] \tag{9}$$

where

$$F(\alpha) = \frac{\sqrt{3}}{2\pi}\int_0^\alpha \frac{dx}{x^{2/3}(1 + x)}$$

Expressing I_d ($R_J = R_2$) in terms of $I_d(I_r \to 0)$ yields

$$I_d(R_J = R_2) = \frac{NI_d(I_r \to 0)}{\beta^{2/3}[1 - F(\alpha)]} \tag{10}$$

$I_d(R_J = R_2)$ can be predicted for all rotation speeds using eq 10 and the value of $I_d(I_r \to 0)$ obtained from a $I_r - I_d$ curve obtained at a relatively slow rotation speed. The value of $F(\alpha)$ for the electrode used is 0.407 and the ratio $N/\beta^{2/3}[1 - F(\alpha)]$ is 0.854.

Results

Determination of *D* in Eq 7. In order to verify that the As(III)–I_3^- system obeys eq 7, I_r–I_d curves were obtained for all values of [As(III)] and ω used in this study. Figure 2 shows a plot of $I_d(I_r \to 0)$ for rotation speeds from 400 to 6400 rpm with [As(III)] = 5.00×10^{-4} *M*. The value of *D* in eq 5 was calculated from Figure 2 to be 0.94×10^{-5} cm^2 sec^{-1}. A plot of $I_d(I_r \to 0)$ for [As(III)] from 0.00 to 1.00×10^{-3} *M* at 2500 rpm was linear and the value of *D* was calculated from the slope to be 0.94×10^{-5} cm^2 sec^{-1}.

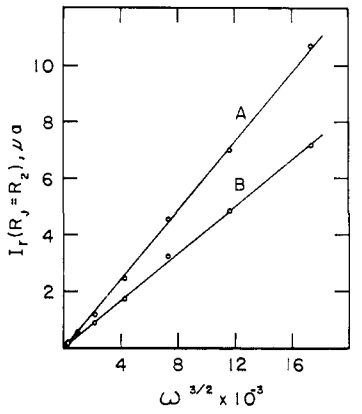

Figure 4. $I_r(R_J = R_2)$ *vs.* $\omega^{3/2}$: curve A, $a_{H^+} = 6.61 \times 10^{-9}$ *M*, [NaI] = 0.070 *M*, $k_{obsd} = 3.27 \times 10^6$ l. mole^{-1} sec^{-1}; curve B, $a_{H^+} = 2.14 \times 10^{-9}$ *M*, [NaI] = 0.100 *M*, $k_{obsd} = 4.88 \times 10^6$ l. mole^{-1} sec^{-1}.

Determination of k_{obsd}. Figure 3 shows I_r–I_d curves ($400 \leq$ rpm ≤ 6400) obtained for $a_{H^+} = 6.61 \times 10^{-9}$ *M* and [I^-] = 0.070 *M* in the absence of As(III), curve A, and for [As(III)] = 1.00×10^{-3} *M*, curve B. Curve A is predicted to be a straight line of slope *N* and zero intercept, and such a result has been obtained previously in the Br_2–As(III) system.[12] In the I_3^-–As(III) experiment, the plot appeared to be linear only for large values of I_d with the result that linear extrapolation from high values of I_d produced a positive intercept on the I_d axis. The "blank titration" (I_d intercept) was 15 ± 3 μA and was observed to be virtually independent of rotation speed, pH, and the rate of change of I_d. Blank titrations were repeated for I_d and I_r axes sensitivities reduced successively by factors of 10 and 100. For each case, the blank titration represented approximately the same percentage of the full I_d scale deflection. No correction was made for this apparent blank titration, the nature of which is unknown.

From the value of $I_d(I_r \to 0)$ obtained from curve B, Figure 3, at 1600 rpm, values of $I_d(R_J = R_2)$ were calculated for all rotation speeds from eq 10, and these values were used to interpret all kinetically controlled I_r–I_d curves.

The remaining curves of Figure 3 show I_r–I_d curves obtained using a ring sensitivity ten times larger than that used for curves A and B.

Figure 4 shows values of $I_r(R_J = R_2)$ plotted *vs.* $\omega^{3/2}$ for two solutions of different a_{H^+} and [NaI]. These slopes are related to the pseudo-second-order forward rate constant for the reaction of As(III) with I_3^- through eq 5. Evaluating the constants in eq 5 for our experimental conditions yields

$$k_{obsd} = \frac{2.02 \times 10^3\omega^{3/2}}{I_r(R_J = R_2)} \tag{11}$$

The calculated values of k_{obsd} for the data shown in Figure 4 are 3.27×10^6 l. mol^{-1} for curve A and 4.88×10^6 l. mol^{-1} sec^{-1} for curve B.

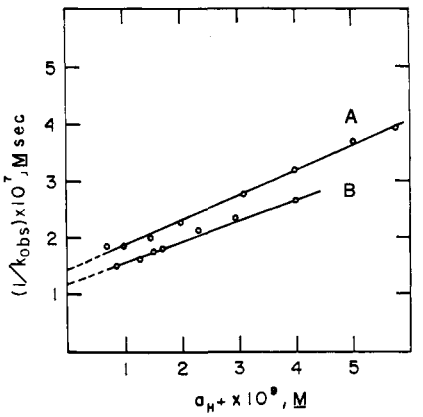

Figure 5. $1/k_{obsd}$ *vs.* a_{H^+}, [As(III)] = 1.00×10^{-3} *M*: curve A, [NaI] = 0.160 *M*, slope = 44.8, intercept = 1.42×10^{-7}; curve B, [NaI] = 0.060 *M*, slope = 37.5, intercept = 1.19×10^{-7}.

Data such as are shown in Figure 4 were obtained over a wide range of a_{H^+} and [NaI] and are described below.

a_{H^+} Dependence of k_{obsd}. Values of k_{obsd} were determined for [As(III)] = 1.00×10^{-3} *M*, [NaI] = 0.060 and 0.160 *M*, and pH from 8.17 to 9.17. It was found that plots of $1/k_{obsd}$ *vs.* a_{H^+} were linear with a nonzero intercept. These results are shown in Figure 5. The values of slope and intercept are given in the legend to Figure 5. k_{obsd} was also determined for two values of pH with $[H_3BO_3] + [H_2BO_3^-] = 0.025$ *M*. These values were identical with those measured for solutions of like pH and $[H_3BO_3] + [H_2BO_3^-] = 0.050$ *M*.

NaI Concentration Dependence of k_{obsd}. Values of k_{obsd} were measured as a function of [NaI] for $a_{H^+} = 2.14 \times 10^{-9}$ and 6.61×10^{-9} *M*. Figure 6 shows the plots of k_{obsd} *vs.* 1/[NaI]. The slopes and intercepts are given in the legend to Figure 6.

Measurement of K_a for H_3AsO_3. The first acid dissociation constant of H_3AsO_3 for $\mu = 0.50$ *M*, $K_a = a_{H^+}[H_2AsO_3^-]/[H_3AsO_3]$, was determined from the titration curve of 1.00 *M* NaH_2AsO_3 with 1.0 *M* $HClO_4$. The pH of the titration solution was measured using a glass electrode standardized as described previously. Water was added to the titration solution so $\mu = 0.50$ *M* at 50% of the equivalence point (pH = pK_a). The value of pK_a determined in this way from three titrations was 8.62 ± 0.01.

Discussion

One reaction mechanism which is consistent with the data shown in Figures 5 and 6 is

$$OH^- + H_3AsO_3 \rightleftharpoons H_2O + H_2AsO_3^- \quad K = K_a/K_w \quad (12)$$

$$I_3^- \rightleftharpoons I_2 + I^- \quad K_1 \quad (13)$$

$$I_3^- + H_2AsO_3^- \longrightarrow \text{products} \quad k \quad (14)$$

$$I_2 + H_2AsO_3^- \longrightarrow \text{products} \quad k' \quad (15)$$

For $[I^-] \gg K_1$, the over-all rate, $-d[As(III)]/dt$, is given by the expression

$$\frac{-d[As(III)]}{dt} = \left\{\frac{k'K_1K_a + kK_a[I^-]}{[I^-](a_{H^+} + K_a)}\right\}[I_3^-][As(III)] \quad (16)$$

$$= k_{obsd}[I_3^-][As(III)] \quad (17)$$

where

$$[As(III)] = [H_3AsO_3] + [H_2AsO_3^-] \quad (18)$$

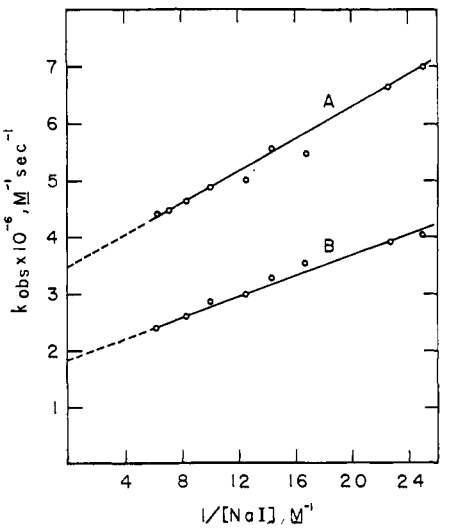

Figure 6. k_{obsd} *vs.* 1/[NaI], [As(III)] = 1.00×10^{-3} *M*: curve A, $a_{H^+} = 2.14 \times 10^{-9}$ *M*, slope = 1.39×10^5, intercept = 3.43×10^6; curve B, $a_{H^+} = 6.61 \times 10^{-9}$ *M*, slope = 0.85×10^5, intercept = 1.85×10^6.

Equation 16 predicts that a plot of $1/k_{obsd}$ *vs.* a_{H^+} is linear having

$$\text{slope} = \frac{1}{K_a}\left\{\frac{[I^-]}{k[I^-] + k'K_1}\right\} \quad (19)$$

and

$$\text{intercept} = \frac{[I^-]}{k[I^-] + k'K_1} \quad (20)$$

The value of K_a can be obtained from the ratio of the intercept to the slope. The values of pK_a calculated for curves A and B of Figure 5 were both 8.50. pK_a was also determined for [NaI] = 0.120 *M* and found to be 8.43. The average value of pK_a is 8.48 ± 0.05. This result is in satisfactory agreement with the value obtained from the titration of NaH_2AsO_3 with $HClO_4$.

Equation 16 predicts that a plot of k_{obsd} *vs.* 1/[NaI] is linear having

$$\text{slope} = \frac{k'K_1K_a}{a_{H^+} + K_a}$$

and

$$\text{intercept} = \frac{kK_a}{a_{H^+} + K_a}$$

K_1 is approximately 1.4×10^{-3} ($\mu \rightarrow 0$),[18] and, to a first approximation, variation in μ will have little effect on K_1. Hence, this value was used to calculate k and k' from the data given in Figure 6. From curve A, $k = 5.6 \times 10^6$ l. mol^{-1} sec^{-1} and $k' = 1.6 \times 10^8$ l. mol^{-1} sec^{-1}, while for curve B, $k = 5.7 \times 10^6$ l. mol^{-1} sec^{-1} and $k' = 1.9 \times 10^8$ l. mol^{-1} sec^{-1}, yielding average results of $k = (5.65 \pm 0.05) \times 10^6$ l. mol^{-1} sec^{-1} and $k' = (1.75 \pm 0.15) \times 10^8$ l. mol^{-1} sec^{-1}.

The largest value of k_{obsd} measured in this work was 7.0×10^6 l. mol^{-1} sec^{-1} for [NaI] = 0.035 *M* and $a_{H^+} = 2.14 \times 10^{-9}$ *M*. Under these conditions, the

(18) W. C. Bray and G. M. J. MacKay, *J. Am. Chem. Soc.*, **32**, 914 (1910).

maximum over-all rate, $-d[As(III)]/dt$, possible at any point in solution is approximately 7 mol $l.^{-1}$ sec^{-1}, and the maximum rate of loss of H_3AsO_3 is 2.8 mol $l.^{-1}$ sec^{-1}.

Chemical kinetic evidence obtained by other methods[19,20] supports the conclusion that reactions 12 and 13 are not rate limiting under our experimental conditions. The forward rate of reaction 12 can be estimated from other hydroxyl-weak uncharged acid reactions. Eigen and Maass[19] report that the forward constant for the reaction

$$OH^- + C_6H_5OH \overset{k_f}{\rightleftharpoons} H_2O + C_6H_5O^-$$

is 1.4×10^{10} l. mol^{-1} sec^{-1} at 25°. The corresponding rate for reaction 12 is probably somewhat faster since H_3AsO_3 has three potentially acidic protons. Hence, we estimate the forward rate constant for reaction 12 to be approximately 4×10^{10} l. mol^{-1} sec^{-1}. Thus, the maximum rate possible for the disappearance of H_3AsO_3 for $a_{H^+} = 2.14 \times 10^{-9}$ M, is approximately 73 mol $l.^{-1}$ sec^{-1}.

The forward and reverse rate constant for the I_3^- dissociation, reaction 13, have been determined by Myers[20] using nmr data. At 35°, he reports $k_f = (7.6 \pm 0.8) \times 10^7$ sec^{-1} and $k_b = (4.1 \times 0.4) \times 10^{10}$ l. mol^{-1} sec^{-1}. Considering the magnitude of these rates, the minor difference in temperature between his and our experiments can be neglected, and it is clear that the I_3^- equilibrium is readily established. Thus, the assumption that reactions 10 and 11 are not rate limiting is valid within experimental error for our experimental conditions.

The experimental value for k is a factor of approximately 30 less than the value obtained for k'. Reaction 12 is an anion–anion reaction while reaction 13 is between an anion and a neutral species, and it seems likely that the difference in k and k' is a result of electrostatic repulsion.

Schenk[21] has suggested a sequence of steps for the I_2–As(III) reaction in alkaline media without discussing the rate-determining step (eq 21–23). A similar

$$I\text{-}I + :As(OH)_2O^- \rightleftharpoons I^- + I\text{-}As(OH)_2O \quad (21)$$

$$I\text{-}As(OH)_2O + OH^- \rightleftharpoons I\text{-}As(OH)_3O^- \quad (22)$$

$$I\text{-}As(OH)_3O^- + 2OH^- \rightleftharpoons I^- + As(OH)O_3^{2-} \quad (23)$$

reaction sequence can be written for the I_3^-–As(III) reaction. Our data indicate that the decomposition of the products formed by the electrolytic attack of I_2 and I_3^- upon $:As(OH)_2O^-$ is the rate-limiting step, *i.e.*

$$I_2 + :As(OH)_2O^- \rightleftharpoons I_2\text{-}As(OH)_2O^- \longrightarrow \text{products} \quad (24)$$

$$I_3^- + :As(OH)_2O^- \rightleftharpoons I_3\text{-}As(OH)_2O^{2-} \longrightarrow \text{products} \quad (25)$$

Acknowledgment. This work was supported by a grant from the University of Minnesota Space Sciences Center under a grant from NASA.

(19) M. Eigen and G. Maass, "Technique of Organic Chemistry," Vol. VIII, Part II, Interscience Publishers, New York, N. Y., 1963, p 1035.

(20) O. E. Myers, *J. Chem. Phys.*, **28**, 1027 (1958).

(21) G. H. Schenk, *J. Chem. Educ.*, **41**, 32 (1964).

Anodic Oxidations of Aromatic Amines. III. Substituted Anilines in Aqueous Media[1]

Jeff Bacon and R. N. Adams

Contribution from the Department of Chemistry, University of Kansas, Lawrence, Kansas 66044. *Received June 3, 1968*

Abstract: The anodic oxidation of a series of *para*-substituted anilines in aqueous media revealed a common pattern of *para*-group elimination and head-to-tail coupling to give 4′-substituted 4-aminodiphenylamines. These products were identified by electrochemical, spectroscopic, and quantitative chemical methods.

In anodic oxidations of aromatic compounds, chemical reactions following electron transfer dominate the over-all electrode process. We have concentrated on this aspect of anodic processes, especially as applied to aromatic amines, in an attempt to establish a general pattern of behavior for this class of compounds. The oxidation pathways of a series of substituted anilines in aqueous solution are summarized herein. Cyclic voltammetry, chronopotentiometry, chronoamperometry, and chemical methods were used to identify the reaction products and to elucidate the mechanism of their formation. The compounds studied were aniline, *p*-anisidine, *p*-phenetidine, *p*-chloroaniline, *o*-toluidine, *p*-aminobenzoic acid, *p*-aminobenzonitrile, and *p*-nitroaniline. They were found to undergo a rapid head-to-tail coupling giving the corresponding 4′-substituted 4-aminodiphenylamine in the oxidized form

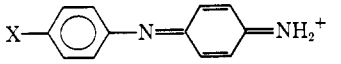

The most extensive previous investigation of anilines was by Wawzonek and McIntyre who found azobenzenes formed upon oxidation in acetonitrile with pyridine present.[2] Mohilner, *et al.*, whose study was restricted to only aniline in strong acid, identified emeraldine-type final products.[3] Both groups postu-

(1) Part II: R. F. Nelson and R. N. Adams, *J. Am. Chem. Soc.*, **90**, 3925 (1968).

(2) S. Wawzonek and T. W. McIntyre, *J. Electrochem. Soc.*, **114**, 1025 (1967).

(3) D. M. Mohilner, R. N. Adams, and W. J. Argersinger, Jr., *J. Am. Chem. Soc.*, **84**, 3618 (1962).